



MAIN RING 2-MAGNET BUMPS

Bruce C. Brown

May 12, 1977

Four sets of 2 magnet (almost) local orbit bumps exist in the main ring. Three of these POS, ANG, and MRV are used to position the beam appropriately for extraction. The fourth is ABORT¹ which is used to locally drive the beam to the main ring abort target. This paper will calculate the elementary properties of such a bump, provide relevant parameters for the bumps presently in use and show measurements of their properties.

Unlike the 3-magnet bumps used at low energy, which can be made exactly local (in a linear machine), these bumps will create finite distortions all around the ring. This is because the positions of ideal phase advance (180° , 360° ...) are usually not available, and furthermore we restrict ourselves to using a single power supply which drives two identical magnets in series. The resulting equal angles will give an ideal bump at the ideal phase only if the β 's of the lattice points are equal. Proper analysis therefore requires accounting for the orbit distortion at the magnets and propagating this distortion plus the bends around the machine lattice.

For an arbitrary 2 bump the solution for the position and slope x , x' at any point between the magnets is given by

$$x = \frac{(\beta_1 \beta)^{\frac{1}{2}} \theta_1}{2 \sin \pi \nu} \cos (\psi - \pi \nu) + \frac{(\beta_2 \beta)^{\frac{1}{2}} \theta_2}{2 \sin \pi \nu} \cos (\psi - 2\pi \nu_{12} + \pi \nu)$$

$$x' = - \left(\frac{\beta_1}{\beta} \right)^{\frac{1}{2}} \frac{\theta_1}{2 \sin \pi \nu} \left[\sin (\psi - \pi \nu) + \alpha \cos (\psi - \pi \nu) \right]$$

$$- \left(\frac{\beta_2}{\beta} \right)^{\frac{1}{2}} \frac{\theta_2}{2 \sin \pi \nu} \left[\sin (\psi - 2\pi \nu_{12} + \pi \nu) + \alpha \cos (\psi - 2\pi \nu_{12} + \pi \nu) \right]$$

for $0 < \psi < 2\pi \nu_{12}$

where β_1, β_2 are the Betatron amplitude² functions at the position of the magnets, θ_1, θ_2 are the bend angles in the magnets, ν is the machine tune, β, α are machine lattice parameters at the point which I calculate x, x' , ψ is the phase advance from the first magnet and $2\pi \nu_{12}$ is the phase advance between magnets. The bend angles at the magnets are assumed to have the relation $\theta = \theta_1 = -\theta_2$ and we calculate x/θ and x'/θ . Note that the formula reduces in the limit $\theta_1 = -\theta_2$ $\nu_{12} = 1$ $\beta_1 = \beta_2$ to the simple formula for an ideal bump:

$$x = (\beta_1 \beta)^{\frac{1}{2}} \theta \sin \psi$$

$$x' = \left(\frac{\beta_1}{\beta} \right)^{\frac{1}{2}} \theta (\cos \psi - \alpha \sin \psi)$$

In order to provide useful information on the bumps I will want to relate the positions and angles not to magnet bend angles but to magnets currents and ultimately to MADC voltages. In order to do this (to a few percent accuracy) I will assume for the magnets that I can calculate the field and bend by a simple excitation formula.

$$\theta = 3.77 \times 10^{-4} \frac{NI(L+G)}{EG}$$

where θ is the bend angle in mr, N is the number of turns, I the current in amps, L the length and G the gap (both in inches) and E the beam energy in GeV. (This is checked for POS by a magnet measurement).³

TABLE I - Bump Magnet Parameters

Name	Magnet Position	Total Phase Advance	Induc. of each Magnet (1kHz)	L Length Inches	MAGNET PARAMETERS					MADC
					G Gap Inches	N Turns	Eθ/I mr GeV Amp	θ/I (400GeV) mr/Amp	I/V Amps/Volt	
POS	F46-A17	349.6°	50mH	40"	1½"	160	1.67	4.17x10 ⁻³	10	
ANG	F44-A15	352.7°	74.8mH	35"	2"	200	1.39	3.49x10 ⁻³	10	
MRV	F47-A18	350.4°	32.8mH	40"	4"	120	.498	1.24x10 ⁻³	10	
ABORT	C46-D17	349.6°	1.2mH	40"	1½"	40	.417	1.04x10 ⁻³	500V/V	

TABLE II - Bump Position and Angle Effects $v=19.45$

Name	Position Calculated	Phase Advance	x/ θ mm/mr	x/I mm/Amp	x'/ θ mr/mr	x'/I mr/amp
POS	ES40	67.8°	93.20	.389	-.1176	.490x10 ⁻³
POS	LAM	91.5°	68.14	.238	.1024	.427x10 ⁻³
ANG	ES40	137.4°	61.18	.214	-1.023	-3.57x10 ⁻³
ANG	LAM	161.2°	17.95	.0626	-1.267	-4.07x10 ⁻³
MRV	LAM	81.5°	109.68	.136	-1.060	-1.31x10 ⁻³

(For MRV $v=19.4$ Calculate Y/ θ , Y/I Y/ θ , Y/I, i.e. vertical deflections

ABORT	C48	66.1°	93.19	.0969	-.11561	-.120x10 ⁻³
	Upstream End					
	of Kicker					
ABORT	C48	71.6°	92.12	.0958	-.11591	-.1205x10 ⁻³
	Downstream End					
	of Kicker					
ABORT	C49	98.8°	68.45	.0712	.0946	+.0984x10 ⁻³
	Abort Target					

To get useful results simply I made a few approximations, including assuming that β, α of the machine are the same at 19.46 as for 19.4 where I have SYNCH outputs (SYNCH - a standard program for synchrotron parameters). Phase advances are simply scaled from the $v=19.4$ results.

In Tables I and II we list the calculated parameters for the quantities which have obvious implications for the machine operation and tuning. Additional useful information on the bump concerns the degree to which they are really local. To see this we must obtain the solution for regions not between the two magnets in the bump.

Now we have

$$x = \frac{(\beta_1 \beta)^{\frac{1}{2}} \theta_1}{2 \sin \pi v} \cos(\psi - \pi v) + \frac{(\beta_2 \beta)^{\frac{1}{2}} \theta_2}{2 \sin \pi v} \cos(\psi - 2\pi v_{12} - \pi v)$$

$$x' = -\left(\frac{\beta_1}{\beta}\right)^{\frac{1}{2}} \frac{\theta_1}{2 \sin \pi v} \left[\sin(\psi - \pi v) + \alpha \cos(\psi - \pi v) \right]$$

$$- \left(\frac{\beta_2}{\beta}\right)^{\frac{1}{2}} \frac{\theta_2}{2 \sin \pi v} \left[\sin(\psi - 2\pi v_{12} - \pi v) + \alpha \cos(\psi - 2\pi v_{12} - \pi v) \right]$$

for $2\pi v_{12} < \psi < 2\pi v$

The external displacements are zero for $\beta_1 = \beta_2, \theta_1 = -\theta_2, v_{12} = 1$ and are small to the extent that these results are approximated. The dominant error term for these bumps goes as $\sin 2\pi v_{12}$ relative to the bump amplitude.

TABLE III - Lattice Parameters Used for the Bumps

Name	Machine Location	Machine Parameters				
		β_1	β_2	ν_{12}	at	ν
POS	F46-A17	91.1	95.5	.9716		19.45
ANG	F44-A15	93.4	93.3	.9772		19.45
MRV	F47-A18	91.7	95.9	.9685		19.43
ABORT	C46-D17	91.0	95.5	.9716		19.46

To confirm these calculations, measurements were taken using the available orbit measurement program. An orbit measurement was stored with all extraction quads and bumps turned off. The tune was measured using the horizontal pinger magnet to be $19.45 \pm .01$. This value was consistent with tune inferred from the values of the extraction quads at that time which would extract resonant beam. Then orbit plots were stored for conditions with one orbit bump turned on at a time

POS with 29 Amps

ANG with 27.5 Amps

MRV with 32 Amps.

These measurements were all taken at 4.6 sec on a 400-GeV ramp or $\sim .12$ sec after flattop begins. The results are shown in Figs. 1, 2, and 3, where the distorted and undistorted orbits are compared. We see that the distortions are indeed local to a large extent. The non-local features are quite visible in the plots but small enough to be operationally unimportant. The rather obvious net orbit shifts are a result of the momentum shift induced by the orbit

distortion at E44 where the rf system seeks to hold the radius fixed. To obtain a quantitative description of these results, the momentum orbit must be taken into account. This quantitative comparison will be left to an appendix.

Use of Extraction Bumps

The function of the extraction bumps is to position both the main ring and extracted beam for minimum losses. MRV is the vertical position bump. Its function is to keep the main ring beam centered in the Lambertson hole (when the beam is pushed to larger radius by POS and ANG). Its angle effect is fairly small and no further tight restrictions exist for the vertical position. It is now connected to drive the beam vertically downward at F49 (opposite to the situation when measurements were taken March 10).

POS and ANG serve to determine the horizontal position and angle of the main ring and extracted beams. There are four constraints on horizontal orbits. First we must avoid hitting the Lambertson magnet septum with either main ring or extracted beam (position and angle - 2 constraints), next we must set the angle of the extracted beam to be parallel to the septum (a restrictive requirement which is critical for losses), finally the step size in the resonant growth of the beam at extraction grows with distance from the stable beam and so the stable beam must be positioned to give a step size appropriate to the 1 cm spacing from wires to cathode on the electrostatic septum. Presently (and for the recent past) the magnets have been connected so that current in POS will increase the radius of the beam at F48 ($\theta > 0$, deflects radially

outward) while ANG is connected to give smaller radii at F48 ($\theta < 0$, deflects radially inward). The resulting deflection and angle at the septum will be given by

$$\Delta x_{ES40}(\text{mm}) = .389 I_{POS} - .214 I_{ANG} \quad (I \text{ in Amps})$$

$$\Delta x'_{ES40}(\mu r) = .490 I_{POS} + 3.57 I_{ANG}$$

We note that the other two horizontal \angle constraints must be provided for by a suitable positioning of the electrostatic septum and Lambertson.

Operationally we might find it useful to try changing POS and ANG together such as to keep Δx or $\Delta x'$ fixed. This can be done with mults on the console as follows:

```
MULT:2    POSITION
          POS
          ANG*-.137
MULT:2    ANGLE
          POS*.55
          ANG
```

Control of MRV, POS, and ANG are primary tools in tuning extraction for minimum losses. Operationally we find that changes of a few amps on any of these supplies (~4 Amps for MRV, ~2 Amps for POS, ANG) will cause significant changes in the observed losses.

References:

1. R. A. Carrigan et al., Main Accelerator Abort System, 1973 Particle Accelerator Conference, IEEE Trans. Nuc. Sci. NS-20, 240, (1973).
2. The formalism is the standard one developed in e.g. E. D. Courand and H. S. Snyder, Theory of the Alternating Gradient Synchrotron, Annals of Physics 3, 1-48 (1958).
3. R. Yamada, private communication, Magnetic Field Measurements on EPB Bump Magnets, January 16, 1974.

APPENDIX

Comparison of Calculations and Data

Detailed comparison of calculated and observed orbits was carried out to determine how careful one needed to be in order to obtain a desired degree of precision. In this appendix I will first compare calculated and measured orbit distortions for POS and MRV and then show results using the approximations that when one changes tune values one can assume that β , α change slowly and that ψ changes can be linearly scaled.

First, here are results for POS and MRV. We will use a SYNCH program which gives parameters at the ends of the quads. (This is near the detector locations except at doublet positions at 49, 11 locations.) Calculations of x/θ will be carried out. Then with the magnet parameters from Table II, we calculate the deflection θ .

POS at 29A gives $\theta = 4.17 \times 10^{-3} \times 29 = .121 \text{ mr}$

MRV at 32A gives $\theta = 1.20 \times 10^{-3} \times 32 = .039 \text{ mr}$.

With this result we directly obtain the results plotted in Fig. 4 for MRV by multiplying by the appropriate x/θ values. But for POS we must account for the momentum shift. We write

$$\Delta x_i = \delta x_i + \eta_i \frac{\Delta p}{p}$$

where δx_i is the Betatron oscillation part of the orbit distortion, η_i is the momentum function, and $\Delta p/p$ the momentum shift. We will evaluate $\Delta p/p$ in two ways. First we simply calculate the orbit distortion at F44 and note that the momentum function should cancel it. We calculate $\delta x_i = -1.03 \text{ mm}$ and find $\eta = 5.286 \text{ m}$ so the momentum shift is

$$\frac{\Delta p}{p} = 1.94 \times 10^{-4}.$$

Alternatively we can add displacements around the ring and note that the betatron amplitudes will add to zero (we exclude the bump region) so

$$\sum \Delta x_i = \sum \eta_i \frac{\Delta p}{p}$$

this yields $\frac{\Delta p}{p} = 1.92 \times 10^{-4}$.

We now calculate and plot values of Δx for POS using both betatron and momentum orbit contributions. The result is plotted in Fig. 4. Note that for these comparisons we have used the calculated deflection directly rather than attempt any fit. We also could be more careful to use precise positions for magnets and position detectors to improve the precision of the calculation.¹ I will assume that the accuracy of the results is sufficient for present use.

Calculational Details

Two more items will be discussed: How much do these results depend on tune and how well can one calculate at one tune value knowing machine parameters at a nearby tune? First, let us compare machine parameters at two tune values. We will compare at several points β and α values for $\nu = 19.4$ and $\nu = 19.45$. Looking at this comparison in Table IV we find that these parameters change about .2% so they will affect only very precise calculations.

TABLE IV

Position	<u>$\nu = 19.4$</u>		<u>$\nu = 19.45$</u>	
	<u>β</u>	<u>α</u>	<u>β</u>	<u>α</u>
A11	104.54	5.722	104.30	5.718
12	29.60	-.573	29.49	-.575
13	95.36	1.858	95.52	1.864
14	28.38	-.589	28.34	-.588
15	97.25	1.840	97.11	1.843

In Fig. 5 we show how a change in tune from 19.4 to 19.45 is reflected in phase advance around the machine. We see that although the phase does not advance linearly at all points, the error due to assuming a linear phase advance is small ($\sim .1^\circ$).

There are other calculational details of significance comparable to these changes. For example, the use of 2 types of quads in the main ring (giving overall only a 2-fold symmetry to the main ring) give differences between sectors of the ring of order 1% in β and 1-2% in α .² Differences between "identical" magnets and in magnet location are also sources of error.

Finally we use this approximation that α , β parameters are unchanged and ψ varies linearly to calculate the sensitivity of the POS and ANG bumps to tune change. In Figs. 7 and 8 we plot position and angle effects at the electrostatic extraction septum ES40 as a function of the machine tune. We observe that the effects are almost linear and small - changing x/θ , x'/θ by only a few percent. We should be insensitive to this for understanding normal operation.

Footnotes

1. Some main ring position detectors are not standard ones and are known to be less reliable. A34 detector is one of these.
2. S. Ohnuma, private communication.

Horizontal Orbit Distortion Due to POS with 29A at 400 GeV/c

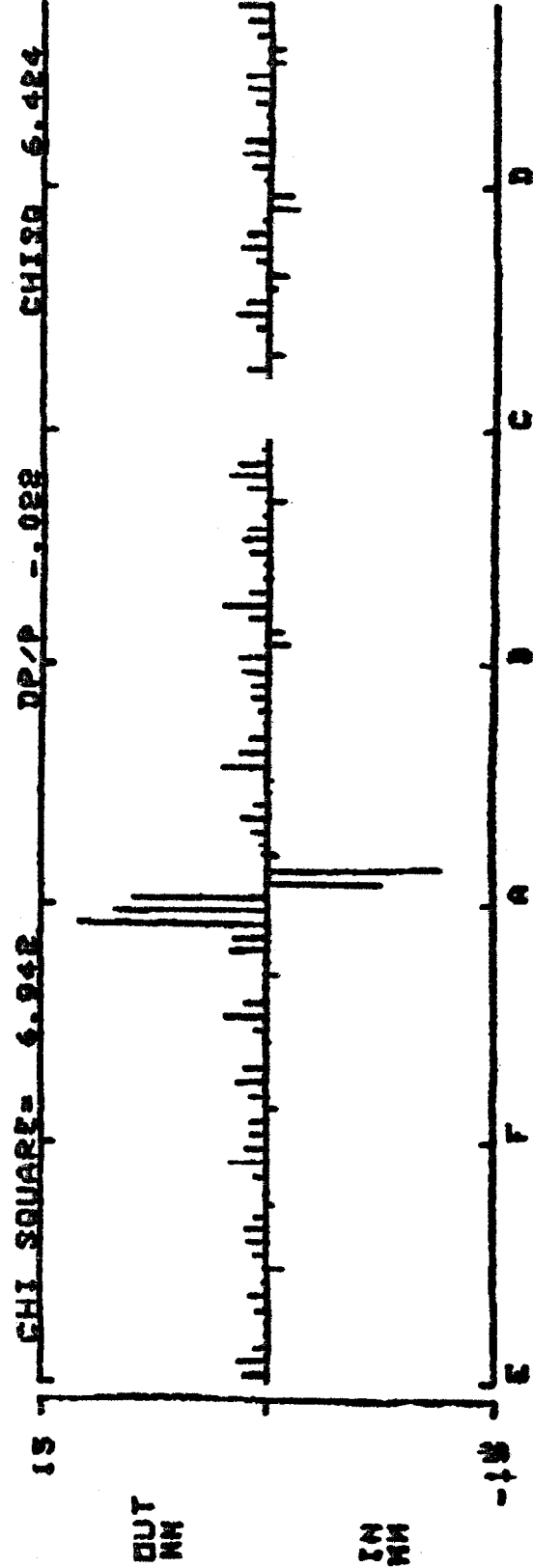
HORIZONTAL CLOSED ORBIT

FILE 1
CALIBRATED
SAMPLE TIME= 4.5
BEND BUS
5020 AMPS
03/09/77 2344

MINUS

FILE 0
CALIBRATED
SAMPLE TIME= 4.5
BEND BUS
5020 AMPS
03/09/77 2341

	F	A	B	C	D
11	1.546	8.907	1.031	0.009	1.164
13	1.951	-7.477	-1.382	-.636	1.078
15	.796	-11.552	-.843	1.149	1.737
17	.094	-1.703	1.078	1.617	1.523
19	-.07	.352	2.976	1.429	-.164
22	-.75	1.031	1.078	-.914	1.211
24	1.193	1.654	-.352	-.047	1.007
26	-.211	-.141	-.107	1.679	1.429
28	-1.054	-.141	1.101	1.992	1.617
32	1.796	3.023	1.3	1.359	-.96
34	1.336	1.804	1.453	-.445	-.96
36	1.453	1.125	-.164	-1.101	-.843
38	-.867	1.094	-.984	0.67	1.453
42	-.258	-.141	1.312	1.828	1.958
44	0.75	2.437	2.414	1.382	1.164
46	2.531	1.148	2.398	-.398	-.703
48	1.359	1.757	.703	-1.734	-.99
49				-1.382	-.117

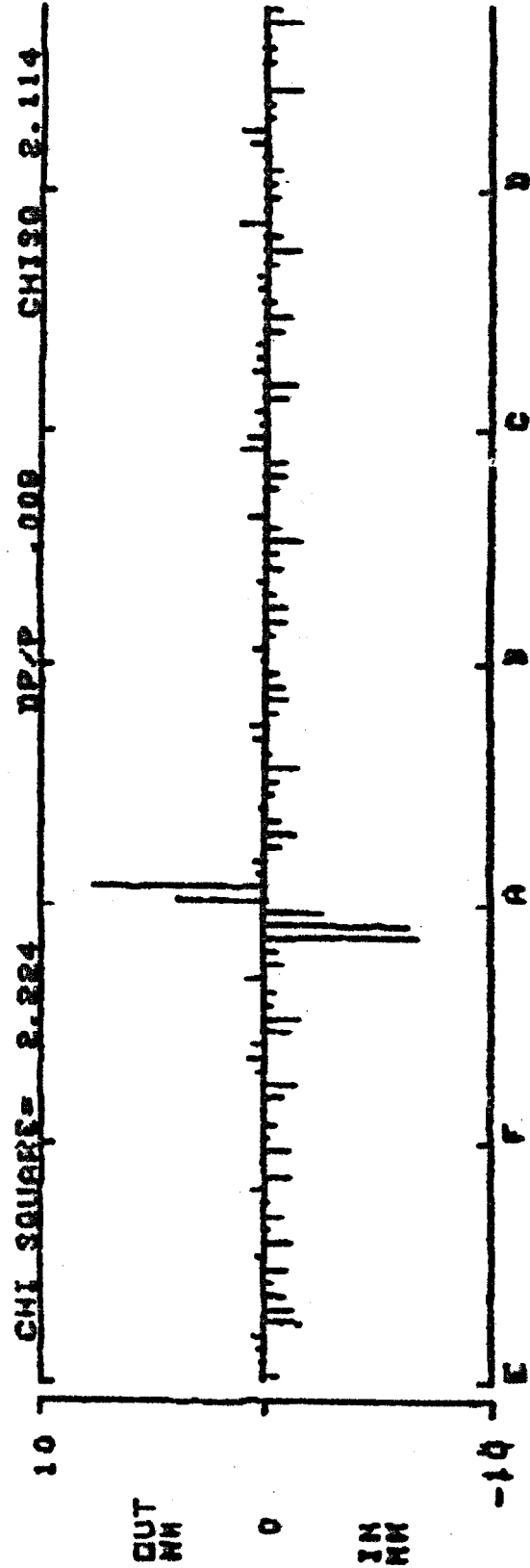


Horizontal Orbit Distortion due to ANG with 27.5A at 400 GeV/c

HORIZONTAL CLOSED ORBIT		<MM> 02/10/77		0010	
FILE #		A	B	C	D
CALIBRATED		3.961	1.07	.281	-.382
SAMPLE TIME=		7.641	.585	.469	-.562
4.5		.398	.258	.867	-.234
BEND BUS		.515	.773	-.1.265	-.686
5020 AMPS		-.609	.927	.373	1.054
02/09/77		-1.312	.375	.252	-.203
		.75	.305	.656	-.281
		.515	.492	-.1.101	-.1.523
		-1.078	-.1.546	.375	-.047
		-1.523	-.492	.258	-.298
		-.258	.796	.375	-.141
		-.445	-.047	.252	-.1.453
		.89	.492	-.1.382	-.562
		.703	.585	.609	-.867
		.515	-.827	1.265	-.023
		-6.82	1.054	.117	-.489
		-6.281	.75	.315	-.1.218
		-2.531			

MINUS

FILE 0	
CALIBRATED	
SAMPLE TIME=	
4.5	
BEND BUS	
5020 AMPS	
02/09/77	



Vertical Orbit Distortion Due to MRV with 32A at 400GeV

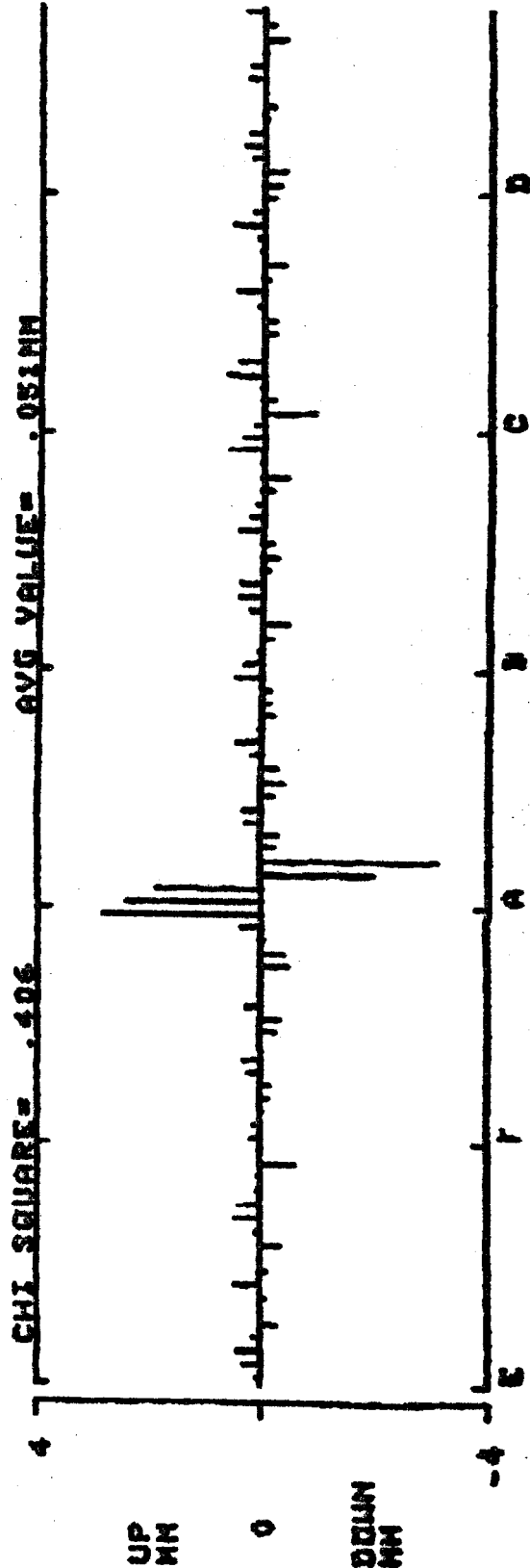
VERTICAL CLOSED ORBIT

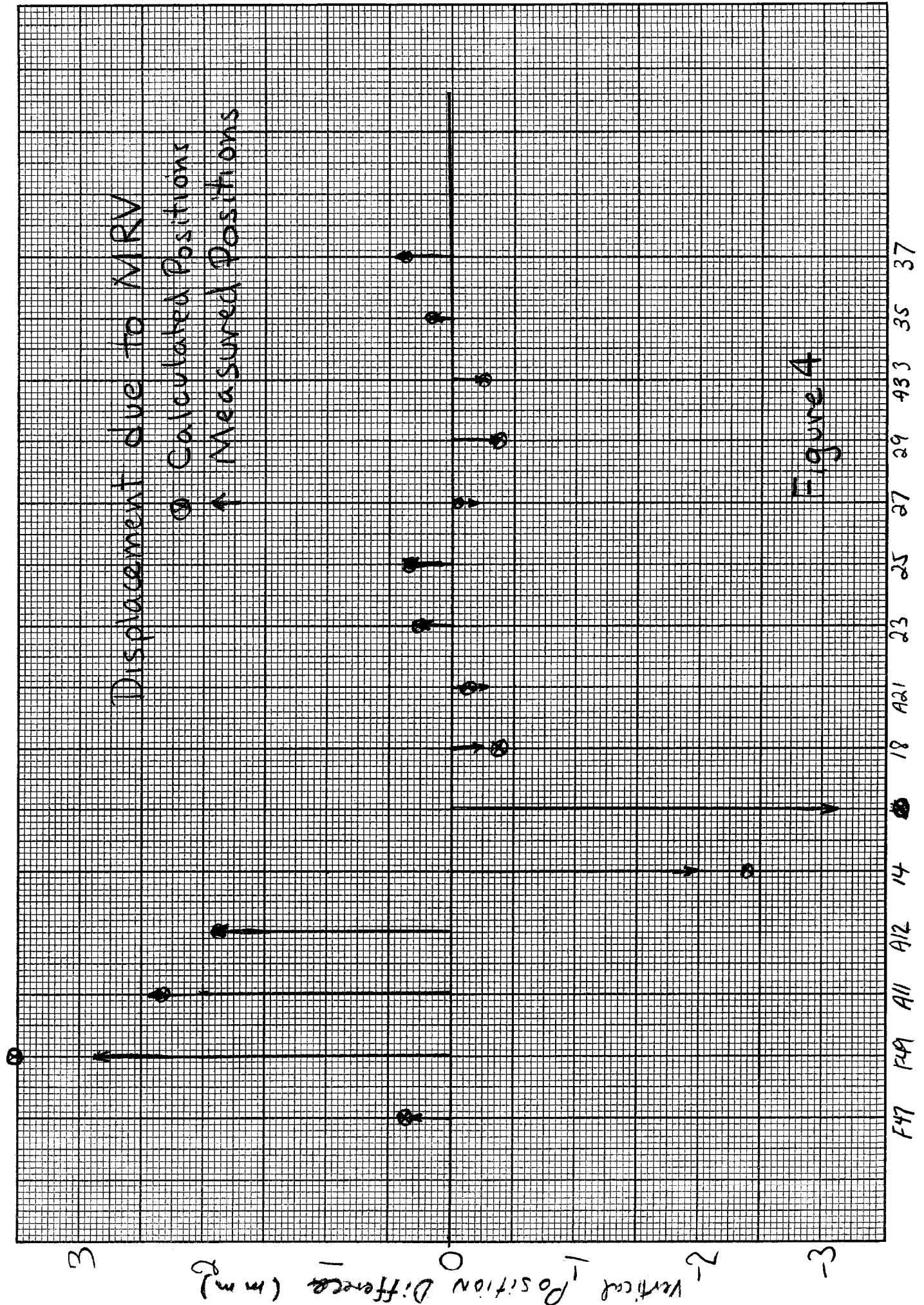
FILE 4
CALIBRATED
SAMPLE TIME= 4.5 SEC
BEND BUS 5020 AMPS
03/09/77 2356

MINUS

FILE 0
CALIBRATED
SAMPLE TIME= 4.5 SEC
BEND BUS 5020 AMPS
03/09/77 2341

	F	E	A	B	C	D
11	167	105	2.443	325	149	201
12	132	281	1.916	397	931	396
14	044	413	-1.986	-176	22	193
16	141	141	-3.102	-421	07	334
18	158	272	-229	229	659	264
21	237	059	-281	439	448	035
23	243	062	352	387	018	176
25	018	457	352	132	185	0
27	295	123	-202	-235	22	29
29	352	009	-264	-158	105	246
33	264	369	-193	429	473	062
35	07	105	166	22	088	378
37	009	466	353	105	378	176
39	492	396	32	211	062	352
43	413	879	-22	-457	114	439
45	07	018	-114	026	553	237
47	343	588	-105	388	193	158
49	2.856	044	483	343	202	185





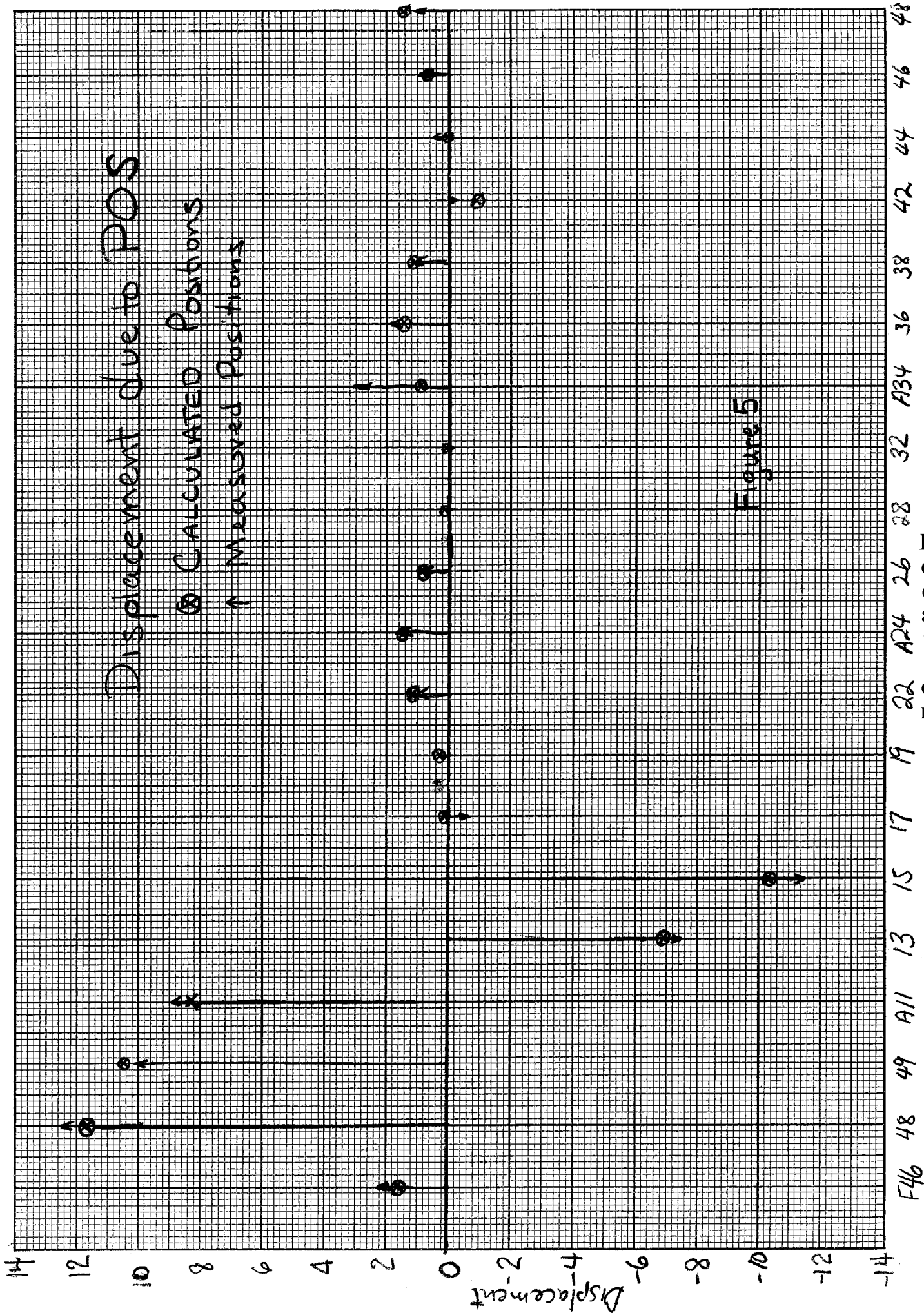


Figure 5

Smoothness of Phase Change.
Machine Tone Change from 19.4 to 19.45
Plot of Change in Phase vs Phase Angle.

$\Delta \Delta (v=19.45) - \Delta \Delta (v=19.4)$

Figure 6

$$\Delta v = \frac{1}{25\pi} (v=19.4)$$

